15th Australasian Fluid Mechanics Conference
The University of Sydney, Sydney, Australia
13-17 December 2004

Flow Structure Around A Finite-Length Square Prism

H.F. Wang[1,2], Y. Zhou[1,#], C.K. Chan[3], W. O. Wong[1] and K.S. Lam[4]
[1] Department of Mechanical Engineering
[3] Department of Applied Mathematics
[4] Department of Civil and Structural Engineering
The Hong Kong Polytechnic University
[2]National Laboratory of Coal Combustion, Huazhong University of Science and Technology
[#]Email: mmyzhou@polyu.edu.hk

Abstract
Turbulent flow structure around a square prism of finite length is experimentally investigated in a closed-circuit low speed wind tunnel. Hotwire and PIV data indicate that the near wake structure is dependent on the aspect ratio of the prism and characterized by vigorous interactions between base and tip vortices when the cylinder aspect ratio is 3 or less, but among spanwise vortices, tip vortices and base vortices at an aspect ratio of 5 and above. The counter-rotating base vortices dominate the near wake close to the prism base and attain maximum vorticity at 1d (prism width) downstream of the prism and decay rapidly downstream. Both the maximum strength and size of these vortices grow with increasing aspect ratio due to weakening interaction between the tip and base vortices. Based on the present data and those in the literature, the flow structure models for different prism aspect ratios are proposed.

Introduction
Flow around bluff bodies with finite length is important and of practical significance in many branches of engineering, such as aerodynamic force on cooling towers, pollutant transport and dispersion around high-rise buildings, forces on under water structures and even heat transfer of printed electronic circuit boards. As such, flow around a finite-length prism has attracted a considerable attention in the literature.

It is now well established that the flow over a finite-length circular cylinder is strongly three dimensional due to the interaction of tip vortex sprung from the free end of the cylinder and the horse-shoe vortex formed at the base (Zdravkovich et al. [15], Okamoto and Sunabashiri [10] and Matinuzzi and Tropea [7]). Etzold and Fielder [2] and Kawamura et al. [4] found that the ratio of cylinder height (H) to diameter (d), i.e., the aspect ratio, has a great influence on the flow structure. When the aspect ratio is less than 4, the wake near the free end of the cylinder is dominated by the down-wash tip vortices, and no periodic Karman vortex shedding occurs. For aspect ratio greater than 4 or 5, alternate Karman vortex shedding occurs along the cylinder except near the free end and the base. More recently, Pattenden et al. [11] investigated the flow structure of tip vortices and horseshoe vortices of a very short cylinder (H/d = 1), and found that the counter-rotating tip vortices move downwards with the descending shear layer, and expand while being advected downstream until attaching the wall at x/d = 2.

Hussein and Martinuzzi [3] carried out flow visualization and LDV measurement of a wall mounted cube in a fully developed channel flow. A reattachment region is formed downstream of the cube by the downwash shear flow originating at the top leading edge. The horseshoe vortex is drawn towards the plane of symmetry up to the reattachment region, and then dispersed outwards by the downwash flow. Krajnovic [5] provided detailed flow visualization of a surfaced-mounted cube and showed a pair of counter-rotating streamwise vortices downstream of the prism base. Lyn et al. [6] studied unsteady turbulent flow around a 2D square prism based on phase-averaged velocities by a two-component LDV. They suggested that, in the base region, the periodic component was governed by the streamwise extent of the vortex formation region, while the turbulent component was governed by the wake width.

In spite of previous investigations, many aspects of the flow structure around a finite-length prism have yet to be better understood. For example, how is the flow dependent upon H/d? How do the tip, spanwise and base vortices interact with each other? This work aims to address these issues and focuses on a finite-length square prism. The aspect ratio examined ranges from 3 to 7. The flow is measured using hotwire and PIV techniques. Based on the experimental data, a schematic flow structure model is proposed.

Experimental Set-up
Fig. 1 shows a schematic diagram of the experimental setup and coordinate system. Experiments were conducted in a closed-loop wind tunnel with a 2.4 m long working section (0.6m × 0.6m). The prism is mounted on a 10mm-thick horizontal flat plate (0.5m × 1.2m) at 30mm downstream of the leading edge. The width, d, of the square prism is 20mm. The cylinder height to width ratio, H/d, is chosen to be 3, 5 and 7. The leading edge was rounded to avoid flow separation. The boundary layer thickness is estimated to be about 2mm at L = 30 mm, resulting in a negligibly small effect on the wake of the prism. The measurements were conducted at a free-stream velocity, U_∞, of 7m/s. The corresponding Reynolds number, Re, based on d is 9,300. The free-stream turbulent intensity is about 0.7%.

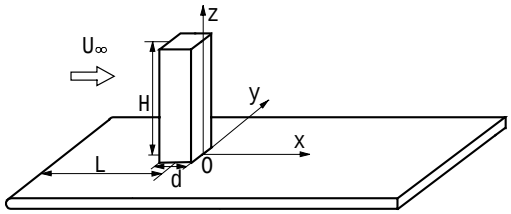

Fig.1 Schematic diagram of the experimental setup.

A single hotwire was placed at x/d = 5 and y/d = 2.5 for various z/d to monitor the dominant frequencies in the wake. A DANTEC particle imaging velocimetry (PIV) was used to measure the flow in the x-z plane at y = 0 and in the y-z plane at x/d = 1, 3 and 5. The CCD camera of the PIV system was placed about 50d downstream of the prism to ensure a negligibly small effect on the near wake of the prism.

Results and Discussion
Dominant vortical structures
In order to investigate the features of the turbulent wake, power spectra of velocities in the x-direction is obtained. Fig. 2 shows the smoothed power spectrum, E_u, of streamwise fluctuating velcoity u at various spanwise locations for the three H/d values. At H/d = 3, there is a broad peak occurring at $f^* = 0.09$, where the asterisk stands for the normalization by U_∞ and d. On the other hand, a pronounced sharp peak occurs at $f^* \approx 0.12$ and 0.13 for H/d = 5 and 7, respectively,

close to that (0.135) of dominant vortices in a two-dimensional (2-D) square cylinder wake, Okajima [9]. The observation suggests that the flow behind the prism of H/d = 5 and 7 may be dominated by spanwise vortices, whereas that at H/d = 3 may not. The present result conforms to the reports by Kawamura et al. [4] and Brede et al. [1] that, when H/d was less than a critical value, 3 to 4, depending on incoming flow condition, no periodic vortex shedding occurred behind the entire prism and the near wake is characterized by the tip vortex generated at the free end and the horse shoe vortex formed at the base of the prism; however, at H/d > 3-4, the periodic spanwise vortex shedding was observed .

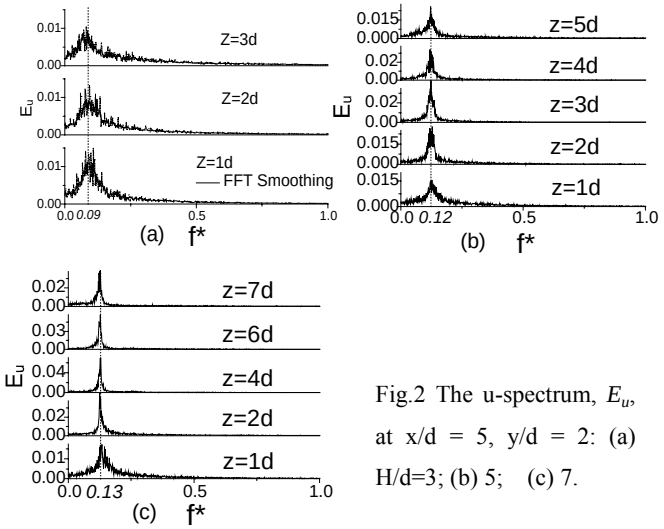

Fig.2 The u-spectrum, E_u, at x/d = 5, y/d = 2: (a) H/d=3; (b) 5; (c) 7.

PIV Measurements

Fig. 3 presents sectional streamlines obtained from the PIV data, averaged from about 200 images, in the (x, z) plane for different H/d, where the reference frame is fixed on the prism. For simplicity, the sectional streamlines are hereinafter referred to as streamlines. The averaged streamlines have been compared with instantaneous ones (not shown) and found to be indeed representative of the typical flow structure. It is evident that the flow structure is qualitatively the same, irrespective of the H/d value. The approaching flow moves upwards, accelerates towards the free end of the prism and then separates from the leading edge.

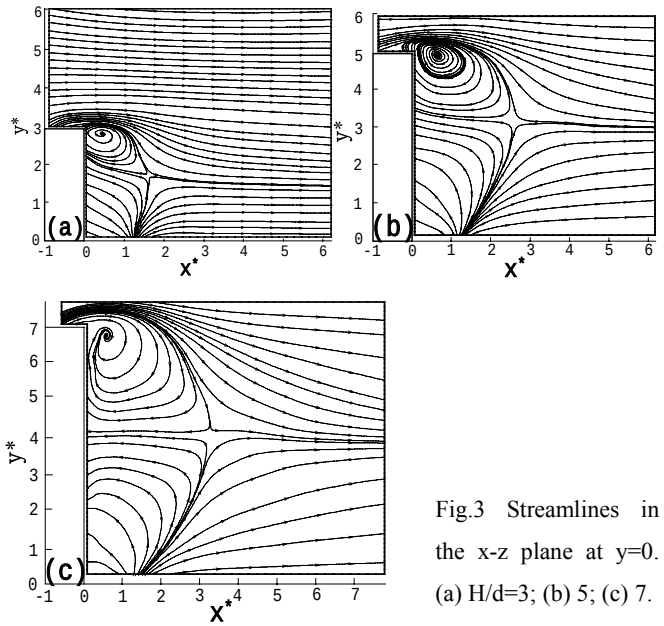

Fig.3 Streamlines in the x-z plane at y=0. (a) H/d=3; (b) 5; (c) 7.

The separated shear layer descends towards the wall while moving downstream. A focus is formed by the downwash flow downstream of the prism free end. In the region near the prism base, the streamlines do not appear affected by the downwash flow separation. This region, along with the downwash flow, grows for a higher H/d. Interestingly, all the streamlines near the prism base merge to a point downstream of the prism. The topology of these streamlines is consistent with the occurrence of a saddle point as illustrated in Fig. 4, which is supported by our oil-film flow visualization results (not shown here). One saddle point is formed near the mid-span downstream of the prism by the downwash flow from the free end and the up-wash flow from the saddle point near the base.

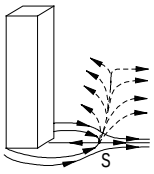

Fig.4 Sketch of the saddle point.

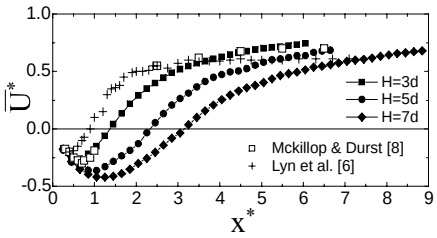

Fig.5 Averaged centerline streamwise velocity measured at mid span of the cylinder.

Figure 5 shows the streamwise velocity $\overline{U}^*$, obtained from the averaged PIV data in the x-z plane, along the centerline at mid-span of the prism, together with Lyn et al.'s [6] and McKillop and Durst's [8] data obtained in the wake of a 2-D cylinder. As H/d increases, the negative $\overline{U}^*$ region grows, indicating that the recirculation zone is increased. At H/d = 3, the up-wash flow appears overwhelming; however, the downwash flow becomes more important for higher H/d. The downwash flow from the free end brings in high speed fluid contributing to the growing recirculation region. Furthermore, both the maximum magnitude of the reversed flow velocity and the length of the recirculation region are larger presently than those in a 2-D cylinder wake. In the 2-D cylinder wake, the end effects are negligibly small, resulting in a smaller recirculation region.

The $\overline{\omega}_x^*$ - contours obtained from the averaged PIV data (200 images) in the y-z plane (Fig. 6) at x/d = 1 display a pair of counter-rotating vortices near the prism base.

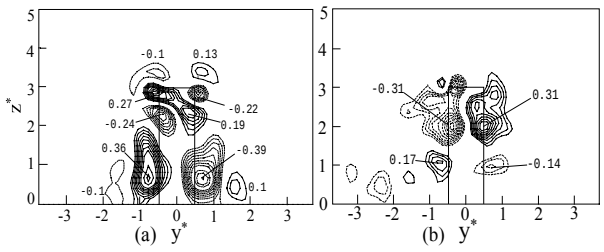

Fig.6 $\overline{\omega}_x^*$ - contours of H/d = 3. (a) x/d =1, (b) 3.

As x/d increases, this pair of vortices (Figs. 6a and 6b) ascends, in consistence with the streamlines in x-z plane (Fig. 3), where the upward moving flow meets the downwash stream from the free end at x/d =1.5 at about the mid-span of the prism. The base vortices decay rapidly in both strength and size. It is worth commenting that the rotational senses of

the base vortices are opposite to those of horseshoe vortices described by Kawamura et al. [4] and Simpson [14]. In fact, this pair of base vortices is surrounded by a pair of weaker vortices, which show the characteristics of horseshoe vortices.

The vorticity distribution near the free end of the prism is quite symmetrical and three pairs of oppositely signed vortical structures are identifiable in Fig. 6a. The upper vortex pair with a peak vorticity of - 0.1 and 0.13 is attributed to the downwash shear layer separating at the leading edge. The other two pairs of vortices occur at the corner of the free end and have larger magnitude of vorticity. Their occurrence is consistent with the flow structure, as illustrated in Fig. 7. This flow structure was numerically observed behind a cube by Saha [13]. The two pairs of vortices occur slightly below the free end, probably due to the downwash shear flow. At x/d = 3, the three pairs of vortices appear to have merged into one pair of higher peak vorticity and larger size. One difference between the tip and base vortices is that the tip vortex grows downstream whereas the base vortex decays rapidly.

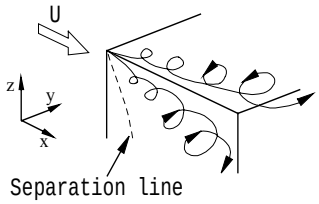

Fig.7 Tip vortex development.

The averaged $\overline{\omega}_x^*$ - contours at x/d = 1 for H/d = 5 (Fig.8a) are rather different from those for H/d = 3 (Fig. 6a). One pair of opposite-signed vortices only occurs near the free end, and the pair of vortices near the base is spanwise stretched considerably. The strength and size of the latter are much larger than those at H/d = 3.

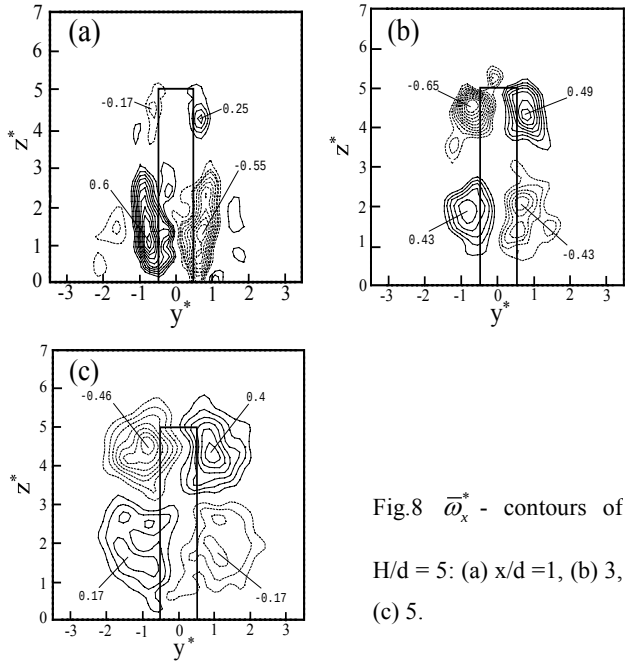

Fig.8 $\overline{\omega}_x^*$ - contours of H/d = 5: (a) x/d =1, (b) 3, (c) 5.

At H/d = 5, the base vortices perhaps develop into the alternately shedding Karman vortices, which are present along most of the prism (Fig. 2b), thus being spanwise stretched at x/d = 1 (Fig 8a). As x/d increases, the vortices decays gradually downstream in the maximum $\overline{\omega}_x^*$, but grow considerably in size, exhibiting one pair of less stretched opposite-signed $\overline{\omega}_x^*$ concentrations. On the other hand, the tip vortices are overwhelmed by the present of spanwise vortices, as confirmed by examining the instantaneous $\overline{\omega}_x^*$ -contours, and consequently display one pair of relatively weak counter-rotating vorticity concentrations near the free end. But they grow downstream in both strength and size, reaching the maximum $\overline{\omega}_x^*$ at x/d = 3 (Fig 8b). At x/d = 5, their size grows larger, though the maximum $\overline{\omega}_x^*$ appears reducing.

The averaged $\overline{\omega}_x^*$ -contours at H/d = 7 (Fig 9) are qualitatively similar to those at H/d = 5. However, there are differences. First, the upper pair of opposite signed concentrations is more spanwise stretched and characterized by a higher vorticity strength at x/d = 1. Like the H/d = 5 case, the maximum $\overline{\omega}_x^*$ increases from x/d = 1 to 3 and then decays slowly downstream. Secondly, the lower pair of vortices are also more stretched and stronger than at H/d = 5. The differences are apparently linked to the enhanced spanwise vortices at a larger H/d.

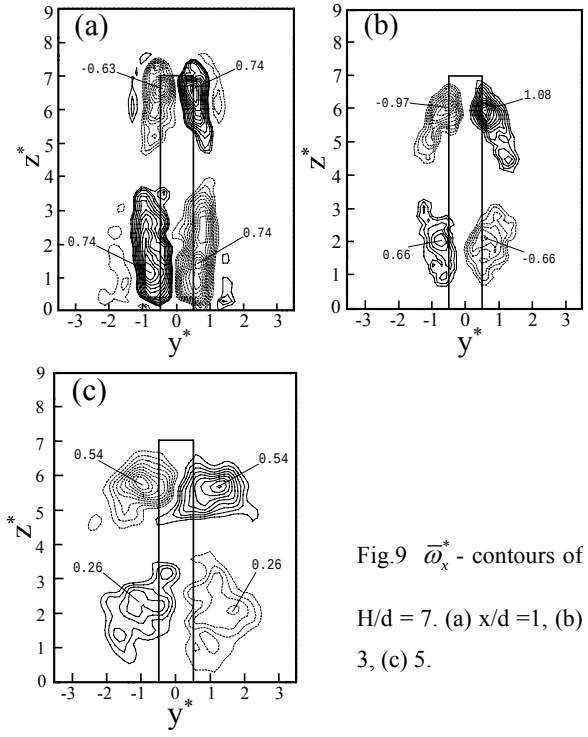

Fig.9 $\overline{\omega}_x^*$ - contours of H/d = 7. (a) x/d =1, (b) 3, (c) 5.

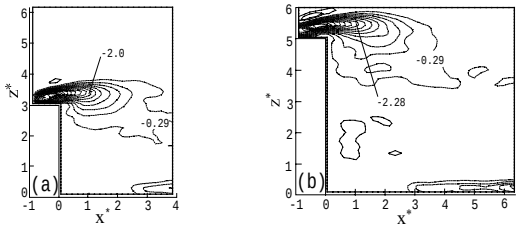

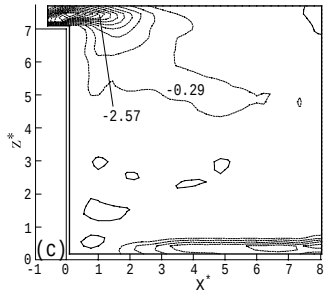

Fig. 10 The $\overline{\omega}_y^*$ - contours: (a) H/d = 3, (b) 5 (c) 7.

The averaged $\overline{\omega}_y^*$ -contours in the x-z plane are presented in Fig. 10. The same scale has been used for the three aspect ratios to facilitate comparison. At H/d = 3, the maximum $\overline{\omega}_y^*$ concentration is – 2.0 and occurs at x/d ≈ 1. As H/d increases, this concentration increases in both magnitude and size, probably due to the diminishing interaction between the tip and base vortices.

Conclusions

The flow around a finite-length prism has been experimentally investigated. The investigation, though preliminary, leads to the following conclusions:

1 At H/d = 3, spanwise vortex shedding is largely suppressed and the near wake is dominated by the tip and the base vortices. At H/d = 5 and 7, periodic spanwise vortex shedding occurs over almost the whole span except very close to the wall. The flow structure is schematically proposed in Fig. 11 for the two cases.

2 While the tip vortex grows in both size and strength downstream, the base vortex decays.

3 The recirculation region grows for a higher H/d probably due to the downwash flow from the free end, which brings in high-speed fluid. However, this region is smallest in a 2-D cylinder case, where the end effects are negligibly small.

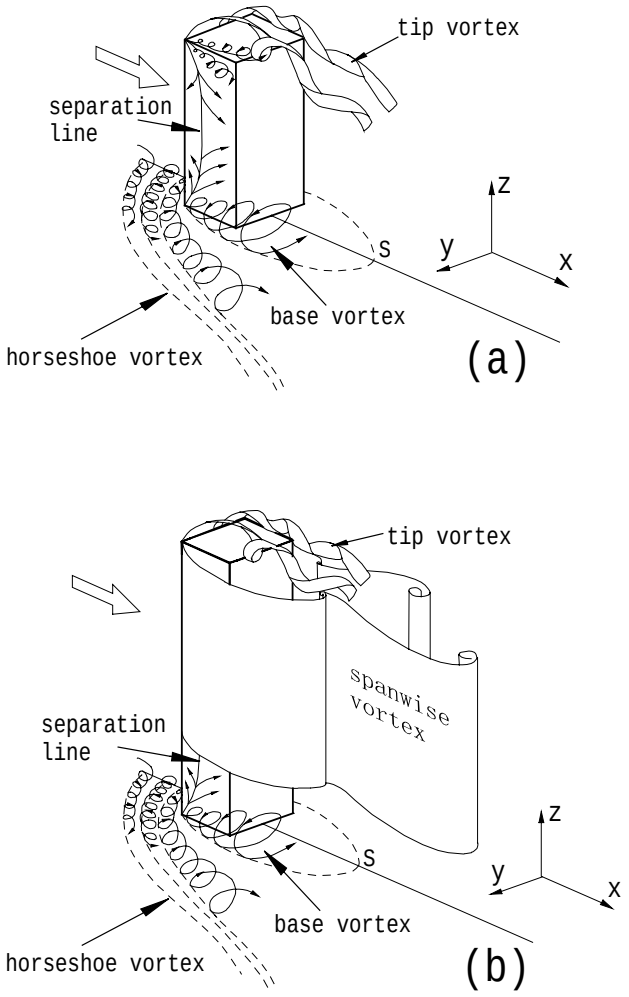

Fig.11 Flow structure behind a square prism:

(a) H/d = 3; (b) H/d ≥ 5.

Acknowledgements

The authors wish to acknowledge the support given to them by the Central Research Grants of The Hong Kong Polytechnic University through Grant G-YD69 and G-T679, and Research Grants Council of HKSAR through grant B-Q862.

References

[1] Brede, M., Eckelmann, H. & Rockwell, D., On the secondary vortices in the cylinder wake, *Phys. Fluids*. **8**, 1996, 2117-2124.

[2] Etzold, F. & Fiedler, H., The near-wake structure of a cantilevered cylinder in cross flow, *Z. Flugwiss.* **24**, 1976, 77-82.

[3] Hussein, H.J. & Martinuzzi, R.J., Energy balance of turbulent flow around a surface mounted cube placed in a channel, *Phys. Fluids*. **8(3)**, 764-780.

[4] Kawamura, T., Hiwada, M., Hibino, T., Mabuchi, I. & Kumada, M., Flow around a finite circular cylinder on a flat plate, *Bull. of JSME*., **27**, 1984, 2142-2151.

[5] Krajnovic, S., Large eddy simulation of the flow around a three-dimensional bluff body, *PhD thesis*, Dept. of Thermo and Fluid Dynamics, Chalmers Univ. of Tech., Gothenburg, Sweden.

[6] Lyn, D.A., Einav, S., Rodi, W. & Park, J.H., A laser-Doppler velocimetry study of ensemble-averaged characteristics of the turbulent near wake of a square cylinder, *J. Fluid Mech*., **304**, 1995, 285-319.

[7] Matinuzzi, R. & Tropea, C., The flow around a surface-mounted prismatic obstacles placed in a fully developed channel flow, *J. Fluid Eng.*, **115**, 1993, 85-92.

[8] McKillop, A.A. & Durst, F., A laser anemometry study of separated flow behind a circular cylinder, *In Laser Anemometry in Fluid Mechanics II*, LADOAN-IST, Lisbon, Portugal 1986.

[9] Okajima, A., Strouhal numbers of rectangular cylinders, *J. Fluid Mech*., **123**, 1982, 379-398.

[10] Okamoto, K. & Sunabashiri, Y., Vortex shedding from a circular cylinder of finite length placed on a ground plane, *JSME Int. J. Ser. II*. **114**, 1992, 512-521.

[11] Pattenden, R.J., Turnock, S.R. & Bressloff, N.W., An experimental and computational study of three-dimensional unsteady flow features found behind a truncated cylinder, *24th Symposium on Naval Hydrodynamics*, Fukuoka, Japan, 8-13 July 2002.

[12] Roshko, A., Perspectives on bluff body aerodynamics, *J. Wind Ind. Aerodyn.*, **49**, 1986, 79-100.

[13] Saha, A.K., Three dimensional numerical simulation of transition flow past a cube, *Physics of Fluids.* **16**, 2004, 1630-1646.

[14] Simpson R.L., Junction Flow, *Annu. Rev. Fluid Mech.*, **33**, 2001, 415-443.

[15] Zdravkovich, M.M., Brand, V.P., Mathew, G. & Weston, A, Flow past short circular cylinders with two free ends. *J. Fluid Mech.*, **203**, 1989, 557-575